JOURNAL OF MATERIALS SCIENCE: MATERIALS IN MEDICINE **16** (2005) 355–360

Effects of silica on the bioactivity of calcium phosphate composites *in vitro*

C. Q. NING, J. MEHTA, A. EL-GHANNAM*
Center for Biomedical Engineering, University of Kentucky, Lexington, 40506, KY, USA
E-mail: aregh2@uky.edu

In the present study, silica-calcium phosphate composites (SiO_2–CaP composites) were developed by mixing the starting materials (SiO_2 and $CaHPO_4$) in different ratios with the addition of 0.1% w/v NaOH solution. The phase composition of the SiO_2–CaP composites was determined by XRD and FTIR. After thermal treatment at 350 °C/1 h and at 1000 °C/3.5 h; all SiO_2–CaP composites composed of β-quartz, α-cristobalite and β-$Ca_2P_2O_7$. The presence of calcium phosphate enhanced the transformation of β-quartz into α-cristobalite at 1000 °C. SEM observation indicated favorable attachment and spreading of neonatal rat calvaria osteoblasts onto the surface of silica-rich SiO_2–CaP composites. After attachment, these cells produced significantly higher amount of protein and expressed higher AP activity than cells attached to silica-poor samples. Results of the study suggested that the silica-based composites are more bioactive than calcium phosphate-based composites. Silica promoted the expression of osteoblast phenotype by both solution-mediated effect and direct interaction with the surface of the substrate.

1. Introduction

Calcium phosphate ceramics, such as hydroxyapatite ($Ca_{10}(PO_4)_6(OH)_2$), tricalcium phosphate ($Ca_3(PO_4)_2$), calcium pyrophosphate ($Ca_2P_2O_7$), have good biocompatibility with human bone tissue and have been widely used as bone graft materials [1–3]. Although widely used, calcium phosphate ceramics may have limited bioactivity due to poor resorbability and in some cases can elicit immunological responses due to high degradation rate [4, 5].

The essential requirement for bioactive artificial biomaterial to exhibit a bone bonding to living bone is the formation of a bone-like apatite layer on its surface in the body environment [6]. On this apatite layer, osteoblasts of living bone can proliferate and produce mineralized extracellular matrix. Many reports [7–9] about the silica-containing bioactive glasses have demonstrated that in aqueous solutions or biological fluids, ion exchanges at the material/solution interface result in the formation of a silica-rich layer, which induces the nucleation and the precipitation of an amorphous calcium phosphate layer on the material surface [1, 7]. To improve the bioactivity of hydroxyapatite ceramics, several attempts [10–15] have been made to prepare hydroxyapatite doped with silica. *In vitro* studies by Gibson *et al*. [15] proved that the incorporation of silicon into the crystal structure of pure hydroxyapatite enhanced the osteoblast-like cell activity. The enhanced bioactivity was attributed to the formation of a poorly crystallized surface apatite layer on silica-substituted hydroxyapatite. Moreover, *in vivo* studies showed enhanced bioactivity and resorbability for silica-substituted hydroxyapatite [16]. The enhanced bioactivity of silica-substituted hydroxyapatite has been attributed to the enhanced material dissolution (resorbability) *in vivo*. Villacampa *et al*. [17] synthesized a hydroxyapatite-silica composite by sol-gel method; structure analyses by SEM and TEM showed that a solid composite material composed a nanometer-scale hydroxyapatite crystalline phase embedded into an amorphous silica matrix can be prepared. However, no further results on the bioactivity of this composite were reported. Berzina *et al*. [18] synthesized HA/SiO_2 and TCP/SiO_2 composites with a mass ratio changing from 5/95 to 40/60 by powder technology and evaluated their mechanical properties; the results showed that the composites with 30 mass% SiO_2 had the maximum mechanical strength. In this study, we attempted to fabricate SiO_2-calcium phosphate composites (SiO_2–CaP composites) with the additive of sodium by powder metallurgy method. The effects of the chemical composition on the crystalline structure of the SiO_2–CaP composites were analyzed. Moreover, the chemical composition and structure were correlated to bone cell activity on the surface of the material.

*Author to whom all correspondence should be addressed.

TABLE I Composition design of the composites

	Composition	
Composite code	$CaHPO_4$ (wt%)	SiO_2 (wt%)
20Si	80	20
40Si	60	40
60Si	40	60
80Si	20	80

2. Materials and method

2.1. Preparation of SiO_2–CaP composites

Commercial SiO_2 (Sigma, 99%, R&D use) and $CaHPO_4$ (Sigma, 98–105%, R&D use) were used as the starting materials. Appropriate ratios of SiO_2 and $CaHPO_4$ powders (Table I) were mixed in polyethylene bottles on a rolling mixer for 20 h. The SiO_2-$CaHPO_4$ mixtures were then moistened with 0.1% w/v NaOH solution and uniaxially pressed into discs (13 mm dia $\times$ 2 mm height) under a pressure of 80 MPa. The discs were subjected to two step thermal treatments at 350 °C/1 h and then at 1000 °C/ 3.5 h in air.

2.2. X-ray diffraction (XRD)

Samples were ground into powders for XRD analyses. The phase composition of the SiO_2–CaP composites was determined on a Rigaku D/Max X-ray diffractometer. Cu K_α radiation was used at the operating condition of 40 kV and 20 mA. The XRD data were collected over the 2θ range of 20–80° with a step size of 0.02°. Identification of phases was achieved by comparing the diffraction patterns of the composites with the standard PDF cards.

2.3. Fourier transform infrared (FTIR) spectroscopy

FTIR analyses were conducted on a Thermo Nicolet Nexus 670 spectrometer (WI, USA). Spectra were collected in the diffuse reflectance mode after 200 scans at 4 cm^{-1} resolution. Samples were prepared by mixing powders of the composites with KBr. Pure KBr was used as a background.

2.4. Cell culture and harvesting

Neonatal rat calvaria osteoblasts (NRCO) were enzymatically isolated using collagenase digestion technique. The calvaria of 1-2-day-old Sprague-Dawley rats were excised, stripped of soft tissue and subjected to a series of four 30-min digestions with 0.2% collagenase in the presence of 0.24 mg/ml of N-*p*-tosyl-L-lysine chloromethyl ketone, a protease inhibitor. The cells from the first digestions were discarded. Cells from the remaining three digestions were pooled, washed, resuspended in α-minimal essential medium (α-MEM) (Gibco, Invitrogen Corp.) supplemented with 10% fetal bovine serum (FBS), 0.1% Penicillin-Streptomycin (Gibco), and 0.06% fungizone (Gibco) and then plated in plastic culture dishes. These cells were used to seed the SiO_2–CaP composite disks. SiO_2–CaP composite samples were sterilized with 70% ethanol and then placed in 12-well plates and seeded with 5×10^4 cells. The cells were left for 15 min on the disc surface to allow for cell adherence, then 2.5 ml TCM was added to each well. Cells seeded on polystyrene culture wells without substrates served as control. The tissue culture plates were incubated 3, 6, 9, 12 and 15 days at 37 °C in a humidified atmosphere of 95% air with 5% CO_2. The medium was exchanged every two days with fresh medium supplemented with 3 mM β-glycerophosphate and 50 μg/mL ascorbic acid.

At the end of each time period the medium was removed and the disks were washed two times with PBS, vortexed in 500 μl 1% Triton-X 100 solution to extract attached cells and extracellular matrix. The tubes containing the cell extract were centrifuged at 1300 RPM for 3 min and the supernatant was collected for measurements of total protein and alkaline phosphatase activity. The extraction procedures were repeated three times to assure complete extraction of cells. The third extraction did not have any measurable values of alkaline phosphatase activity. Therefore, for all samples, the supernatants of the first and second extractions were mixed together and used for total protein analysis and alkaline phosphatase activity measurements.

2.5. Total protein analysis

The protein concentration in the triton-X extract was determined using the BCA Protein Assay Reagent Kit (Pierce Biotechnology) employing a UV visible spectrophotometer (Genesys^{TM} 10 Spectrophotometer, Thermo Spectronic) at 562 nm. This method combines the well-known reduction of Cu^{2+} to Cu^{1+} by protein in an alkaline medium with the highly sensitive and selective colorimetric detection of the cuprous cation using a unique reagent containing bicinchoninic acid. Calibration curve was obtained by measuring the absorbance of a series of standards with known protein concentration in 1% Triton-X.

2.6. Alkaline phosphatase (AP) specific activity

Quantitative AP activity was determined by an assay based on the hydrolysis of *p*-nitrophenylphosphate (*p*-NPP) to *p*-nitrophenol (*p*-NP). AP activity is expressed as nmol of *p*-NP/ml/min. 300 μL of the unknown extract were added to the working reagent containing *p*-nitrophenylphosphate (Sigma 104, Sigma-Aldrich Corp.). The release kinetics of AP in the unknown sample was determined using a UV visible spectrophotometer (Genesys^{TM} 10 Spectrophotometer, Thermo Spectronic) at 410 nm. The AP specific activity was calculated by dividing the AP activity by its corresponding total protein concentration.

2.7. Cell morphology

After various culture periods, the medium was removed and the discs with attached cells were washed with PBS

twice, fixed in glutaraldehyde for 3–4 h and dehydrated in graded ethanols (30–100%) and freon. The fully dried samples were coated with a thin gold film and the morphology of the cells was analyzed by scanning electron microscopy (SEM, Hitachi S-3200).

2.8. Gene expression

MC3T3-E1 cells were used for the gene expression experiments. 100 μL of MC3T3-E1 cell suspension containing (approximately 3.4×10^6 cells) were seeded onto the surface of each SiO_2-CaP composite sample as described in Section 2.4. Cells seeded on polystyrene culture dishes served as control. After 12 days in culture, attached cells were washed and lysed using 200 μL TRIzol reagent (Invitrogen Life Technologies). Total RNA was isolated, purified and reverse transcribed into cDNA using the SuperScript™ First-Strand Synthesis System. cDNA was then amplified using the Platinum® *Taq* DNA Polymerase kit (Invitrogen life technologies) for 36 cycles of 2 min at 94 °C, 45 s at 55 °C, and 45 s at 72 °C. In order to verify the PCR products, 15–20 μL of the amplified cDNA were electrophoresed on a 2% agarose gel containing ethidium bromide. RNA samples were analyzed for the expression of osteonectin (OSN).

3. Results

3.1. XRD

Our previous results showed that the original SiO_2 and $CaHPO_4$ powders composed of β-quartz and monetite, respectively [19]. XRD analyses in the present study revealed that all the SiO_2-CaP composites were composed of β-quartz (PDF # 46-1045), α-cristobalite (PD F #39-1425) and β-$Ca_2P_2O_7$ (PDF #9-346). The XRD patterns of the SiO_2─CaP composite are shown in Fig. 1. It is interesting to note that while the diffraction intensities of β-quartz and α-cristobalite increased with the increase of silica content, the ratio of $I_{(101)\alpha\text{-cristobalite}}/I_{(101)\beta\text{-quartz}}$, which represents the relative content of α-cristobalite and β-quartz, varied independent of the silica content. For the composites with 20–60% silica content, the ratios increased with the increase of silica content, however, the ratio for the composite with 80% silica was lower than that for 60Si. The $I_{(101)\alpha\text{-cristobalite}}/I_{(101)\beta\text{-quartz}}$ ratios for 20Si, 40Si, 60Si and 80Si are 0.72, 0.9, 1.21 and 0.97, respectively.

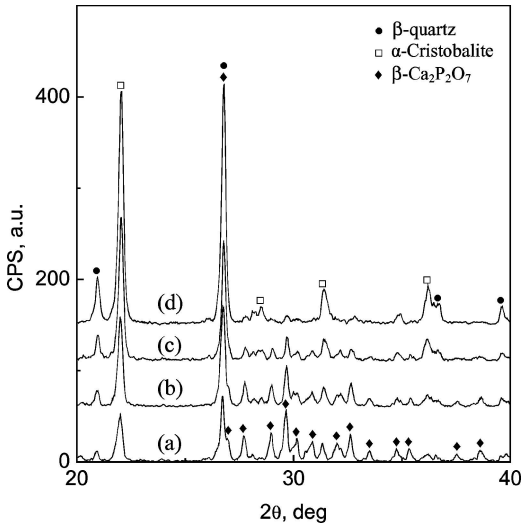

Figure 1 XRD patterns of SiO_2─CaP composites, (a) 20Si, (b) 40Si, (c) 60Si, (d) 80Si. The crystalline phases for all the SiO_2─CaP composites are β-$Ca_2P_2O_7$ (PDF #9-346), β-quartz (PDF #46-1045) and α-cristobalite (PDF #39-1425).

3.2. FTIR

FTIR spectra of the SiO_2─CaP composites are shown in Fig. 2. The assignments of the FTIR spectra of the SiO_2─CaP composites are according to the references [20–23]. The asymmetric terminal P─O stretching bands of β-$Ca_2P_2O_7$ appear at 1188, 1158, 1140, 1102, 1088, 1069 cm^{-1}. The bands at 1054, 1046, 1029, 1003 cm^{-1} are attributed to the symmetric terminal P─O stretching mode of β-$Ca_2P_2O_7$. The bands for asymmetric bridge P─O stretching mode appeared at 975, 946, 920 cm^{-1}. The band at 727 cm^{-1} is due to the symmetric stretching vibration of the bridge P─O bonds. The bands at 613, 567, 540, 527, 455 cm^{-1} are due to the asymmetric bending vibrations of terminal P─O bonds. The bands for symmetric bending vibrations of P─O bonds present at 588 and 527 cm^{-1}, the latter overlapped with one of the asymmetric bending vibration bands of P─O. The Si─O─Si asymmetric stretching bands present at 1160, 1127, 1063 cm^{-1}. While, the bands for Si─O─Si bending mode appear at 800, 781, 524, 477 cm^{-1}. The sharp band at 695 cm^{-1} is most probably due to the vibrations of six-membered rings [23]. All the peaks for calcium phosphate decrease in intensity with the increase in Si content. Whereas, the peaks due to β-quartz increased in intensity gradually.

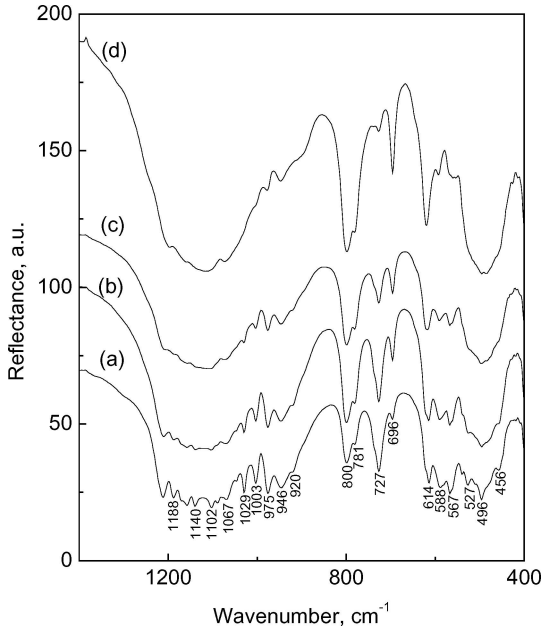

Figure 2 FTIR spectra of SiO_2─CaP composites, (a) 20Si, (b) 40Si, (c) 60Si, (d) 80Si. The intensities of the bands for β-$Ca_2P_2O_7$ at 455, 496, 511, 528, 540, 567, 585, 613, 727, 920, 946, 975, 1003, 1029, 1046, 1054, 1069, 1088, 1102, 1140, 1158, 1170, 1188 cm^{-1} decreased with increasing silica content, whereas, those of the bands for silica at 477, 524, 696, 781, 800, 1063, 1127, 1160 cm^{-1} increased. The shoulder at 622 cm^{-1} is the characteristic band of α-cristobalite.

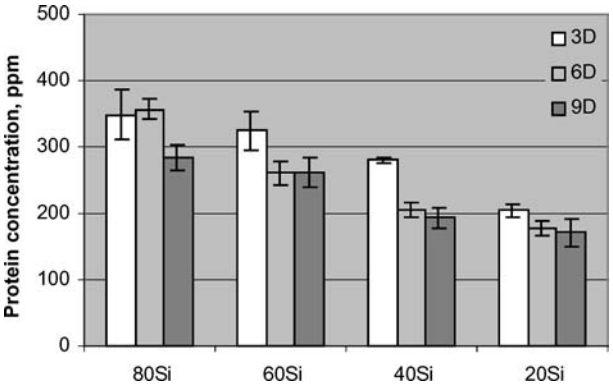

Figure 3 Total protein concentrations of the SiO_2–CaP composites after various culture periods. The total protein concentration increased gradually with the increase of Si content. Except for 80Si, the total protein concentrations of all the other samples decreased slightly with the increase of culture time, however, the differences were not statistically significant ($P > 0.05$, $n = 3$).

3.3. Total protein analysis

Fig. 3 shows the total protein extracted from the SiO_2–CaP composite discs after various culture periods. With the increase of Si content, the total protein concentration increased gradually, which indicated that silica promoted the protein synthesis. Except for 80Si, the total protein concentrations of all the other samples dropped slightly with the increase of culture time, however, the differences were not statistically significant ($P > 0.05$, $n = 3$).

3.4. AP specific activity

Fig. 4 shows the alkaline phosphatase specific activity expressed by cells attached to SiO_2–CaP composites after various culture periods. The specific AP activity of the cells cultured on the SiO_2–CaP composites increased with the increase of culture time. The AP activity results also indicate that silica enhanced the differentiation of NRCO. After all time periods, cells attached to silica-rich composites expressed significantly higher alkaline phosphatase activity than cells attached to silica-poor samples ($P < 0.05$, $n = 3$). Moreover, statistical analysis indicated that there was no significant difference between 40Si and 20Si in terms of AP activity.

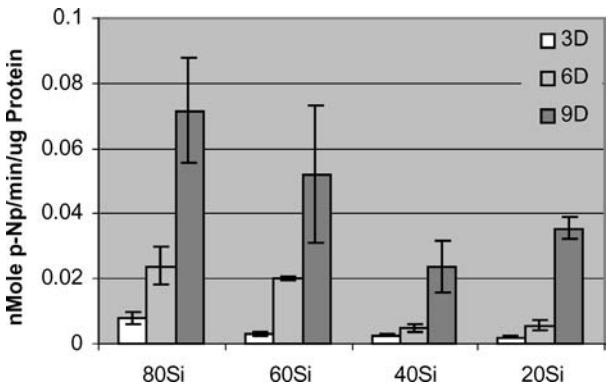

Figure 4 AP specific activities of the SiO_2–CaP composites after various culture periods. The specific AP activity of the cells cultured on the SiO_2–CaP composites increased with the increase of culture time. After all time periods, cells attached to silica-rich composites expressed significantly higher alkaline phosphatase activity than cells attached to silica-poor samples ($P < 0.05$, $n = 3$). There was no significant difference between 40Si and 20Si in terms of AP activity ($P > 0.05$, $n = 3$).

3.5. Morphology observation

The SEM-EDX analyses indicated that silica-rich composites significantly enhanced cell adhesion and spreading. Fig. 5 shows surface morphologies of the SiO_2-CaP composites seeded with 50,000 NRCO cells after 7 days in culture. Cells attached to the surface of 20Si were spread and produced plenty of extracellular matrix (ECM) which made the material particles connect each other. Interestingly, many tiny crystals (100 nm) were scattered on the cell membrane and the ECM. EDX analysis showed that these particles are Ca-P rich phase. With the increase of silica content, the cell attachment and spreading were enhanced. While uncovered areas were seen on the surface of 20Si, the surface of the 40Si was fully covered by attached cells. The surface of 80Si was covered by a sheet of cell layer which was fully spread on the surface. In addition, it can be observed that many sphere particles presented on the surface of 80Si composite; EDX analysis showed that these particles are Si rich phase.

3.6. Gene expression

Fig. 6 showed the OSN expression by MC3T3 E1 cells attached to different SiO_2–CaP composite samples after 12 days in culture. OSN band (108 bp) can be seen for all the SiO_2–CaP composites. Cells attached to polystyrene culture dishes did not express OSN mRNA.

4. Discussion

Results of our study showed that silica-rich calcium phosphate composite enhanced protein synthesis and AP activity of neonatal rat calvaria osteoblasts. Structure analyses using XRD and FTIR showed that the variation in the chemical composition does not affect the crystalline phases of the SiO_2–CaP composites after treatment at 1000 °C. β-$Ca_2P_2O_7$, β-quartz and α-cristobalite were detected in all samples. However, in conjunction with the variation in the chemical composition we observed a variation in the $I_{(101)\alpha\text{-cristobalite}}/I_{(101)\beta\text{-quartz}}$ ratio. This variation could be due to the variation of silica content and the enhancement effect of calcium phosphate phase on the transformation of β-quartz to α-cristobalite. Samples containing less than 40% calcium phosphate resulted in a decrease in the crystallization of α-cristobalite. Previously, we showed that, in SiO_2–CaP composites prepared without NaOH, α-cristobalite was only formed after treatment at 1200 °C [19]. Therefore, in the present study, the enhancement of the transformation of β-quartz into α-cristobalite at 1000 °C could be attributed to the synergistic effect of NaOH and the longer dwell time.

Earlier studies in the literatures [12, 18] reported the formation of $Ca_3(PO_4)_2SiO_4$ after thermal treatment of

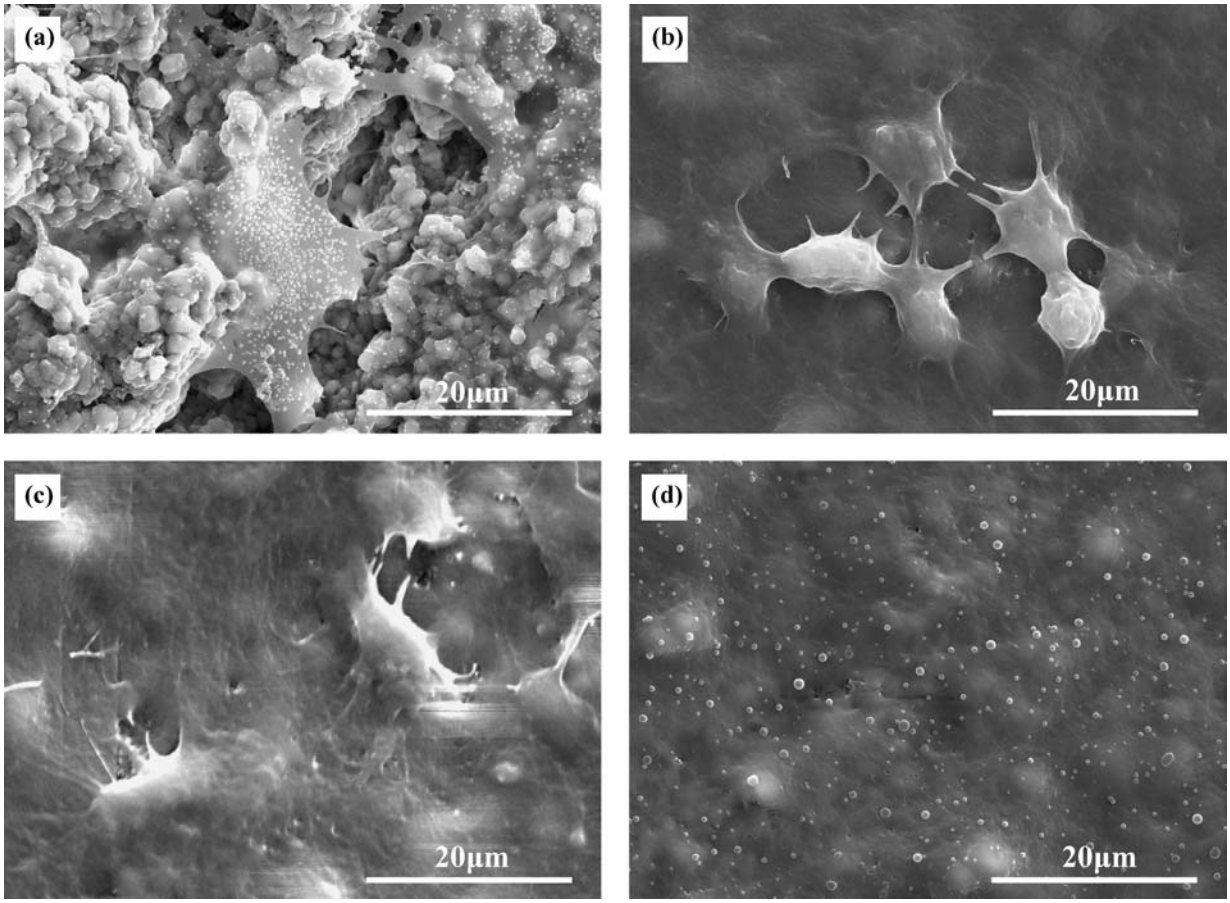

Figure 5 Surface SEM images of the SiO_2─CaP composites seeded with 50,000 NRCO cells cultured for 7 days (a) 20Si, (b) 40Si, (c) 60Si, (d) 80Si. Uncovered areas were seen on the surface of 20Si. With the increase of silica content, the cell attachment and spreading were enhanced. The surface of 80Si was covered by a sheet of cell layer which was fully spread on the surface. Many tiny Ca, P-rich crystals were scattered on the cell memberane and the extracellular matrix on the surface of 20Si (a) and Si-rich spherical particles were observed on the surface of 80Si composite (d).

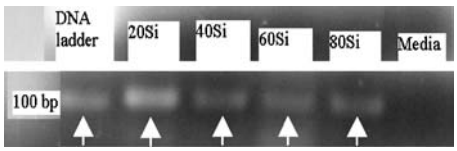

Figure 6 Osteonectin (OSN) expression by MC3T3 E1 cells attached to SiO_2─CaP composites and polystyrene culture dish after 12 days culture. The primers sequence for mRNA amplification was GGAGCAGGACATCAACAAG (forward) and TAAACAAGGGGGTAGTGGAAG (Reverse). OSN bands at about 108 bp can be seen for all the SiO_2─CaP composites. No OSN band was observed for the control cells.

hydroxyapatite-silica-composite at 1100 °C. However, in our studies, no calcium phosphate silicates were detected in the SiO_2─CaP composites probably because the starting materials were different. During the sintering process, sodium can migrate into grain boundaries or incorporated in crystal lattice defects of silica and calcium phosphate. However, because the concentration of sodium was very little, XRD and FTIR analyses could not detect this modification. No significant shifts were detected in the XRD patterns and FTIR spectra. On the other hand, we observed minimal effect of SiO_2 on calcium phosphate phase transformation. This is in contrary to data in the literature which showed that incorporation of more than 3.32 weight percentage of silicon into the structure of HA will result in decomposition of the latter [10]. The incorporation of magnesium will destabilize the structure of hydroxyapatite and favors its thermal conversion into β-tricalcium phosphate [12]. On the other hand, Langstaff *et al*. showed that substitute of silicon for phosphorus resulted in the stabilization of α-tricalcium phosphate [24]. In our study, no measurable effect of silica on the crystalline structure of calcium phosphate was detected probably because the processing parameters was not sufficient to enhance the incorporation of silicon into the calcium phosphate crystalline structure.

The variation in the chemical composition of the SiO_2─CaP composites greatly affected bone cell attachment, protein synthesis and AP activity. SEM analyses showed more bone cells attached and spread on the surface of silica-rich samples. After attachment, these cells produced higher amount of protein and expressed elevated level of AP activity. Morevoer, osteonectin gene was expressed only by cells attached to the SiO_2─CaP composites. The intensity of OSN band for 20Si appeared to be higher than that of other samples due to the differences in cellular activity on the surface of the composite samples. Si-rich composites have strong stimulatory effect on bone cells, therefore, after 12 days, the time point at which the expression of OSN was evaluated, cells on the surface of the Si-rich composites may have down regulated OSN formation and proceeded into the mineralized tissue formation stage. Cells attached to the plastic culture dish did not express

any of the osteoblast phenotypic markers. The protein synthesis and enzyme release are complex processes, which may be affected by many factors. In this study, the protein concentration slightly decreased as the culture period increased, which implied that the protein synthesis is a major cell function in the early days of culture. Other cell differentiation activities may replace protein synthesis with the increase of culture time. AP activity significantly increased with the increase of culture duration. High AP activity is an important marker for bone cell differentiation and has been widely used for initial screening of the bioactivity of bone implant materials. It is interesting to note that the significant increase in protein synthesis and AP activity was associated with the increase in silica content in the composite. Cells attached to samples containing 80Si produced double the concentration of protein and AP enzyme compared to that produced by cells attached to 20Si. Previous studies have shown that silicon plays an important role in the surface bioactivity of silica-based bioactive glasses [7–9]. In the physiological environment (pH = 7.4), silica should be negatively charged due to its lower isoelectric point and surface silanols (Si─OH) will be generated [25]. These Si─OH groups will bind to various functional groups of proteins via hydrogen bonding and long-range electrostatic ionic amine bonds (─Si─O─$^{+}H_3N$─) [26] and thus produce a favorable surface environment for cells to attach. The SEM analysis (Fig. 5(a)) showed that many small Ca─P rich crystals formed on the surface of 20Si composite, and many spherical silicon-rich particles formed on the surface of 80Si composite (Fig. 5(d)). These Ca─P rich and Si-rich particles may be produced by the reprecipitation of Ca, P and Si ions in the medium resulted from the corrosion of the SiO_2─CaP composites. This suggested that Si ions were released from the silica-rich composites during culture periods, so it is possible that some Si─OH groups formed on the surface of silica-rich composites, which will enhance the protein adsorption and synthesis, and provide a favorable surface for cells to attach. In addition, many reports in the literature have shown that silicon is very important to bone formation and growth at *in vitro* and *in vivo* conditions [27]. In this study, the attached cells on the silica-rich composites produced higher AP activity, which implied that silica promoted the expression of osteoblast phenotype by direct interaction with the surface of the substrate. Furthermore, we speculate that the silicon released from the Si rich substrate has contributed to the enhancement of cell differentiation by a solution-mediated effect.

5. Conclusions

After thermal treatment at 1000 °C for 1 h, the crystalline phases of the SiO_2─CaP composites were independent of the silica content. Calcium phosphate enhanced the transformation of β-quartz to α-cristobalite, while, minimal effect of SiO_2 on calcium phosphate phase transformation was observed in this study. More bone cells attached and spread on the surface of silica-rich samples. After attachment, these cells produced higher amount of protein and expressed higher AP activity. Silica-based ceramic is more bioactive than calcium phosphate-based ceramic.

References

1. W. P. CAO and L. L. HENCH, *Ceram. Inter.* **22** (1996) 493.
2. J. S. SUN, Y. H. TSUANG, C. J. LIAO, H. C. LIU, Y. S. HUANG and F. H. LIN, *J. Biomed. Mater. Res.* **37** (1997) 324.
3. T. KASUGA, M. SAWADA, M. NOGAMI and Y. ABE, *Biomaterials* **20** (1999) 1415.
4. S. R. RADIN and P. DUCHEYNE, *J. Biomed. Mater. Res.* **27** (1993) 35.
5. N. KIVRAK and A. C. TAS, *J. Am. Ceram. Soc.* **81** (1998) 2245.
6. L. L. HENCH, *ibid.* **81** (1998) 1705.
7. L. L. HENCH and J. WILSON, *Science* **226** (1984) 630.
8. T. KOKUBO, *J. Non-Cryst. Solids* **121** (1989) 138.
9. T. KOKUBO, H. M. KIM and M. KAWASHITA, *Biomaterials* **24** (2003) 2161.
10. S. R. KIM, D. H. RIU, Y. J. LEE and Y. H. KIM, *Key Eng Mater* **210–220** (2002) 85.
11. I. R. GIBSON, S. M. BEST and W. BONFIELD, *J. Biomed. Mater. Res.* **44** (1999) 422.
12. S. R. KIM, J. H. LEE, Y. T. KIM, D. H. RIU, S. J. JUNG, Y. J. LEE, S. C. CHUNG and Y. H. KIM, *Biomaterials* **24** (2003) 1389.
13. F. BALAS, J. PEREZ-PARIENTE and M. VALLET-REGI, *J. Biomed. Mater. Res.* **66A** (2003) 364.
14. A. J. RUYS, *J. Aust. Ceram. Soc.* **29** (1993) 71.
15. I. R. GIBSON, K. A. HING, S. M. BEST and W. BONFIELD, in 12th International Symposium on Ceramics in Medicine, edited by H. Ohgushi, G. W. Hastings, and T. Yoshikawa, Nara, Japan, 1999, p. 191.
16. N. PATEL, S. M. BEST, W. BONFIELD, I. R. GIBSON, K. A. HING, E. DAMIEN and P. A. REVELL, *J. Mater. Sci. Mater. Med.* **13** (2002) 1199.
17. A. I. VILLACAMPA and J. M. GARCIA-RUIZ, *J. Cryst. Growth* **211** (2000) 111.
18. L. BERZINA, R. CIMDINS, D. VEMPERE and I. KNETS, *Key Eng. Mater.* **206–213** (2002) 1587.
19. C. Q. NING, Y. GREISH and A. EL-GHANNAM, *J. Mater. Sci. Mater. Med.* **15** (2004) 1227.
20. H. A. ELBATAL, M. A. AZOOZ, E. M. A. KHALIL, A. S. MONEM and Y. M. HAMDY, *Mater. Chem. Phys.* **80** (2003) 599.
21. Z. WU, K. LEE, Y. LIN, X. LAN and L. HUANG, *J. Non-Cryst. Solid* **320** (2003) 168.
22. V. VINCENT, C. BREANDON, G. NIHOUL and J. R. GAVARRI, *Eur. J. Solid State Inorg. Chem.* **34** (1997) 571.
23. M. SITARZ, M. HANDKE and W. MOZGAWA, *Spectrochimica Acta* **56A** (2000) 1819.
24. S. D. LANGSTAFF, M. SAYER, T. J. N. SMITH and S. M. PUGH, *Mater. Res. Soc. Symp. Proc.* **550** (1999) 1727.
25. D. T. HUGHES WASSELL and G. EMBERY, *Biomaterials* **7** (1996) 859.
26. K. D. LOBEL and L. L. HENCH, *J. Biomed. Mater. Res.* **39** (1998) 575.
27. E. M. CARLISLE, *Science* **167** (1970) 279.

Received 2 March
and accepted 19 October 2004